SLAC-PUB-179
December 196

SIMILARITY OF SHIELDING PROBLEMS AT ELECTRON AND PROTON ACCELERATORS*

H. DeStaebler

Stanford Linear Accelerator Center
Stanford University, Stanford, California

(First Symposium on Accelerator Radiation Dosimetry and Experience, Brookhaven National Laboratory, November 3-5, 1965)

*Work supported by U.S. Atomic Energy Commission.

1. INTRODUCTION

The aim of this paper is to stress the similarities between the shielding problems at a high energy, high beam power electron accelerator and those at a high energy proton accelerator. For this viewpoint to be fruitful the shielding of the electron-photon cascade must not dominate, and here is where the restrictions of high energy and high power come in. If the machine has high power, then the shield must be thick and a penetrating component may dominate even though it has low intensity at the source. If the energy is high, then significant numbers of penetrating neutrons (with energies above a few hundred MeV) are produced, and these may control the shielding. At very small forward angles muons may dominate, if the maximum range exceeds the shield thickness--just as in the case of high energy proton accelerators.

In an electron-photon cascade in copper a few-tenths percent of the initial energy goes into photonuclear reactions, and this fraction decreases as Z increases. In the transverse direction the electron-photon cascade spreads much less than the nuclear component which almost always controls the transverse shielding. In the forward direction the electron-photon cascade may penetrate significantly in a low Z shield, like earth or ordinary concrete, but a modest amount of medium or high Z material will cause the nuclear cascade (or the muons) to dominate.

Thus, outside a thick shield the radiation fields are similar at electron and proton machines, so the dosimetry and skyshine problems are similar. Duct streaming problems may be quite different, however, especially since the hydrogenous plugs which are effective for fast neutrons are frequently inefficient for photons.

2. ELECTRON-PHOTON CASCADE

Analytic shower theory[1,2] accounts for the main features of the longitudinal or one-dimensional development of the electron-photon cascade. Usually for shielding calculations the behavior at great depths is needed where approximations in the theory may have important consequences. Few experiments go deeper than 15 or 20 radiation lengths[3,4,5] (denoted by X_o), but these and simple theory agree that the shower decreases exponentially with an absorption mean free path of several radiation lengths. This agreement may be accidental, however, because the most penetrating component, which one would expect to control the shower at great depths, consists of photons with energies near the minimum in the interaction cross section[28] (hence with the greatest mean free path, denoted by Λ), and in most analytic shower theory there are approximations that eliminate this minimum in the photon cross section. Fig. 1 shows that Λ varies from about $2\ X_o$ at low Z to about $4\ X_o$ at high Z. Scattering, which decreases the effective absorption length in a real three-dimensional shower, is more important at high Z because the average electron energy is lower, and an absorption mean free path around $3\ X_o$ is reasonable for all Z. Fig. 1 shows that λ, the nuclear removal mean free path, is at least about twice the photon removal mean free path.

A useful quantity in calculations of photon induced reactions in the cascade shower is the total path length traversed, anywhere in the shower, by all photons with energy in (k, dk). In Approximation A of shower theory[1] this quantity, called the differential photon track length, is

$$\frac{d\ell}{dk} = 0.57 \frac{E_o X_o}{k^2} \tag{1}$$

where E_o is the energy of the incident electron. Monte Carlo calculations[6] show that Eq.1 is accurate over a wide range of k, and that it exceeds the true value for k near E_o or near the critical energy, ϵ_o.

The radial or transverse spread requires three-dimensional shower theory which is too complicated to be done very accurately analytically, so Monte Carlo calculations are useful.[8,9] Experiments are complicated by the requirements of a large dynamic range in the detector and of small sizes for the incident beam and the detector.[3] For shielding applications a useful way to summarize the Monte Carlo results is to consider the energy absorbed per unit volume, dw/dv. Define the fraction of the energy absorbed beyond radius a by

$$U(a) = \frac{1}{E_o} \int_{r=a}^{\infty} \int_{z=o}^{\infty} \frac{dw}{dv} 2\pi\, r\, dr\, dz \tag{2}$$

U is shown in Fig. 2 with a measured in units of X_1 which are determined empirically so that the various calculations form a universal curve. For water X_1 is chosen to coincide with the Moliere unit of length[10], X_m, which is the characteristic measure for the radial distributions in analytic shower theory

$$X_m = X_o \frac{E_s}{\epsilon_o} \tag{3}$$

where E_s is a constant equal to 21.2 MeV. In summary

Material	$X_1(g/cm^2)$	$X_m(g/cm^2)$ (ref.7)
H_2O	10.6 ref. 9	10.6
Al	13.4 ref. 9	12.9
Cu	15.6 ref. 9	14.7
Pb	21.5 ref. 8	18.4

In high Z the shower spreads somewhat more than the simple theory indicates. These values of X_1 are shown in Fig. 1.

For shielding purposes the behavior of U at large a is of interest, but unfortunately in Fig. 2 neither the exponential nor the curve derived from shower theory at shower maximum (at s = 1 in the usual notation [1,10]) looks like a good model for extrapolation. As a practical matter it is usually possible to put a small high Z shield close to the sides of the target to absorb most of the electron-photon cascade that leaks out.

3. NEUTRONS

The procedure outlined here for calculating the photonuclear shielding is fairly simple. It is basically the same as that first used for reactor shielding, and in many details it is a direct application of the scheme developed by Moyer and co-workers and applied to the 184 inch cyclotron and to the Bevatron.[11,12]

Fig. 3 shows the general layout and defines some symbols. The radiation level from a point source at a point P on the outside surface of the shield is

$$D_P = \frac{1}{r^2} \int F(T)\, B(T) \exp[-H(\theta)/\lambda(T)] \frac{d^2n(T,\theta)}{dT\, d\Omega}\, dT \qquad (4)$$

T	neutron kinetic energy
r	distance from target to P
F	biological conversion factor (rem/n cm^{-2})
H	shield thickness
λ	effective removal mean free path
B	buildup factor so that $B \exp(-H/\lambda)$ represents the tail of the nuclear cascade
$\frac{d^2n}{dT\, d\Omega}$	yield of neutrons into (T, dT) and $(\theta, d\Omega)$ arising from the absorption of an electron beam with current I and energy E_o.

At low energies $B \approx 1$ and F is well calculated;[13] at high energies $BF \equiv G$ may be taken from the work of Neary and Mulvey.[14]

Eq. 4 may be written

$$D_P = \frac{1}{r^2} \sum G_i \exp(-H/\lambda_i) \frac{dn_i}{d\Omega} \qquad (5)$$

where the subscript i denotes a range of neutron energies for which G and λ are fairly constant and

$$\frac{dn_i}{d\Omega} = \int_{T_i}^{T_{i+1}} \frac{d^2n}{dT\, d\Omega}\, dT \qquad (6)$$

Moyer approximated the sum in Eq. 5 by a single term, (since below a couple of hundred MeV λ decreases rapidly as T decreases[12,15]), with $\lambda = 158\ g/cm^2$ which is typical of the effective removal mean free path for neutrons with energies above several hundred MeV, and with

$$\frac{dn(\epsilon,\theta)}{d\Omega} = \int_{\epsilon}^{T_{max}(\theta,\, E_o)} \frac{d^2n}{dT\, d\Omega}\, dT \qquad (7)$$

with ϵ = 150 MeV.

The distribution in angle and energy of photoneutrons has not been measured extensively above roughly 100 MeV. In an approximate calculation fictitious two-body reactions replace the actual complicated reactions.[16] Then

$$\frac{d^2n}{dT\,d\Omega} = I \int \frac{N_o}{A} \frac{d\sigma(k,\theta^*)}{d\Omega^*} \frac{\partial(k,\theta^*)}{\partial(T,\theta)} \frac{d\ell}{dk}\,dk \tag{8}$$

I	incident electron current
N_o, A	Avogadro's number, atomic weight
$\frac{d\sigma}{d\Omega^*}$	Assume isotropy in the center of mass so this equals $\sigma_{total}/4\pi$.
$\frac{\partial(k,\theta^*)}{\partial(T,\theta)}$	Jacobian from variable transformation
$\frac{d\ell}{dk}$	differential photon track length, Eq. 1.

The total cross sections are shown in Fig. 4. For thin shields the giant resonance reactions dominate; these have been studied extensively[17,18,19]. For thick shields the pion reactions[20] are most important. The pseudodeuteron reaction [17] always contributes but never dominates. The $1/k^2$ variation of the photon track length makes the neutron yields insensitive to the behavior of the cross section at higher energies. Preliminary measurements [21] up to 5 BeV are consistent with σ_{total} roughly constant at the order of 100 mb/nucleon, and there is some evidence that σ_{total} decreases at very high energies.[22]

The two-body approach of Eq. 8 gives reasonable agreement with the measured spectra of photoprotons with $50^\circ \leqslant \theta \leqslant 94^\circ$ from 950 MeV bremsstrahlung on copper.[16] Fig. 5 shows $d\sigma/d\Omega$ (essentially Eq. 7 from Eq. 8) for electrons on copper for ϵ = 100, 150, 200 MeV. Also shown is Moyer's $dn/d\Omega$ per 6.3 BeV proton interacting in copper for ϵ = 150 MeV. The two 150 MeV curves have similar shapes; for equal incident beam powers the neutron yield from protons is about 400 times greater than from electrons. Note that for electrons $dn/d\Omega$, and hence D, is proportional to $I\,E_o$, the incident beam power, and to X_o (via $d\ell/dk$).

Figure 6 shows $r^2 D_p$ derived from Fig.5 and Eq.5 with five energy groups and Moyer's curve for $\lambda(T)$.

Some comments on this whole procedure may be appropriate.

a) This approach is sometimes called "semi-empirical" because λ is determined from experiment, and although $dn/d\Omega$ and G are based on reasonable, approximate calculations, various measurements indicate that there are no gross errors.

b) In the model implied by Eq. 4 and Fig. 3 there is no spreading of the nuclear cascade in the shield. All of the spreading arises from the angular distributions of the neutrons from the source. These approximations are better the more uniform the shield thickness, and the greater the separation between target and shield.

c) Since the cascade is taken to be one-dimensional ("straight ahead" approximation), λ should be derived from a bad geometry experiment.

d) Empirically λ scales with the inelastic σ at high energies and with the total σ at low energies.[12] These cross sections vary approximately[23] as $A^{3/4}$, so for different materials λ is proportional to $A^{1/4}$ (in which case the effective A of $S_i\,O_2$ is 20.2) and this is the variation of λ shown in Fig.1.

e) Most of the radiation field at the outer surface of the shield consists of low energy particles, the secondaries in equilibrium with the penetrating, high energy particles. These secondaries have a broad angular distribution so that simply replacing r by $r + r'$ in Eq. 4 may not give a good estimate of $D_{P'}$, the radiation level at P' (see Fig. 3). A better procedure is to treat the surface of the shield as a new source by integrating D_P over the surface of the shield and letting it reradiate according to some new angular distribution, for example, isotropic into 1 or 2π, or cosine.

As an example of the application of all this, Fig. 7 compares measurements made at CEA[24] with the present method of calculation. The points are the levels actually measured with a Bonner sphere dosimeter (uncorrected for background) at four points outside the shield. The calculation is based on: a rough interpolation between the 45° and 90° curves on Fig. 6; a factor of 0.5 to take account that the dosimeter only measures part of the level; the level at the surface of the shield is integrated over (multiplied by) 2 steradians and reradiated isotropically into one-quarter of a sphere with a radius of 10 feet. Considering the crudeness of this estimate, the agreement is amazingly close.

4. MUONS

Muons are readily photoproduced by ordinary Bethe-Heitler pair production. Several reasonable assumptions make possible a simple calculation of the differential energy spectrum of muons arising from the absorption of an electron of energy E_0.

At high energies the total muon pair cross section per radiation length is approximately

$$\sigma(k) = \frac{7}{9}\left(\frac{m}{\mu}\right)^2 \frac{\ln k/\mu}{\ln 183/Z^{1/3}} \tag{9}$$

where m is the rest energy of the electron and μ that of the muon. Assume that the energy distribution of the produced muons is constant from 0 to k; this will overestimate somewhat the yield near $E_\mu \approx k$. The differential spectrum is

$$\frac{dn}{dE_\mu} = 2 \int_{E_\mu}^{E_0} \sigma(k) \frac{d\ell}{dk} \frac{dk}{k} \tag{10}$$

where the factor of 2 arises because there are two muons per pair. The integral spectrum is

$$n(E_\mu) = \int_{E_\mu}^{E_0} \frac{dn}{dE_\mu} dE_\mu \tag{11}$$

and it is shown in Fig. 8 as a function of E_μ/E_0. Also shown is the yield of muons from a high energy proton beam (taken from Fig. XII-9 of reference 25) which is richer at lower energies partly because lower energy pions are more likely to decay.

For muons the production and absorption[26] mechanisms are rather well known. A fairly unique range is associated with each energy. At electron and proton machines the high energy muons are peaked predominantly in the forward direction because in pair production and in nuclear pion production the transverse momenta are on the order of μ, and muons are rarely a problem for transverse shielding.[16] In a thick shield multiple scattering[27] introduces a spread comparable with that arising from the initial angular spread so both effects should be combined in arriving at a muon flux.[25]

REFERENCES

1. B. Rossi, High-Energy Particles, Prentice-Hall, New York, 1952.

2. S. Z. Belenkii and I. P. Ivanenko, Cascade Theory of Showers, Soviet Phys.-Uspekhi, 2 : 912 (1960).

3. Y. Murata, Investigation of Cascade Showers in Lead with X-Ray Films, J. Phys. Soc. Japan, 20 : 209 (1965).

4. G. Backenstoss, B. D. Hyams, G. Knop and U. Stierlin, A Total Absorption Scintillation Detector for Electrons, Photons and Other Particles in the GeV Region, Nucl. Instr. and Meth. 21 : 155 (1963).

5. W. Blocker, R. W. Kenney and W. K. H. Panofsky, Transition Curves of 330-MeV Bremsstrahlung, Phys. Rev., 79 : 419 (1950).

6. C. D. Zerby and H. S. Moran, Studies of the Longitudinal Development of Electron-Photon Cascade Showers, J. Appl. Phys., 34 : 2445 (1963)

7. O. I. Dovzhenko and A. A. Pomanskii, Radiation Units and Critical Energies for Various Substances, Soviet Phys. - JETP, 18 : 187 (1964)

8. H.-H. Nagel, Elektron-Photon-Kaskaden in Blei, Z. Physik, 186 : 319 (1965).

9. C. D. Zerby and H. S. Moran, Oak Ridge National Laboratory, personal communication, 1963.

10. K. Greisen, Extensive Air Showers, in Progress in Cosmic Ray Physics, Vol. III, North-Holland, Amsterdam, 1956.

11. B. J. Moyer, Evaluation of Shielding Required for the Improved Bevatron, USAEC Report UCRL-9769, Lawrence Radiation Laboratory, June 1961.

12. R. Wallace, Shielding and Activation Considerations for a Meson Factory, Nucl. Instr. and Meth. 18, 19 : 405 (1962).

13. Protection Against Neutron Irradiation Up to 30 MeV, National Bureau of Standards Handbook 63, November 1957.

14. Protection Against Electromagnetic Radiation Above 3 MeV and Electrons, N Neutrons and Protons, p. 4, ICRP Publication Publication 4, Pergamon, London, 1964.

15. Shielding for High-Energy Electron Accelerator Installations*, National Bureau of Standards Handbook 97, July 1964. *, i.e., 100 MeV and below.

16. H. De Staebler, Transverse Radiation Shielding for the Stanford Two-Mile Accelerator, USAEC Report SLAC-9, Stanford Linear Accelerator Center, November 1962.

17. A. Wattenberg, Nuclear Reactions at High Energy, in Encyclopedia of Physics, Vol. XL, Springer, Berlin, 1957.

18. M. E. Toms, Bibliography of Photo- and Electronuclear Disintegrations, Bibliography No. 24, U. S. Naval Research Lab., Washington, D. C., July 1965.

19. Photonuclear Reactions, Bibliographical Series No. 10, International Atomic Energy Agency, Vienna, 1964.

20. C. E. Roos and V. Z. Peterson, Photodissociation of Complex Nuclei at Energies between the Mesonic Threshold and 1150 MeV, Phys. Rev. 124 : 1610 (1961)

21. H. R. Crouch et al, Gamma-Ray Proton Interactions between 0.5 and 4.8 BeV, Phys. Rev. Letters, 13 : 636 (1964).

22. H. S. Murdoch and H. D. Rathgeber, Evidence for Energy Dependence of Photon-Nucleon Cross section from Cosmic Ray Experiments, Physics Letters, 13 : 267 (1964).

23. S. J. Lindenbaum, Shielding of High-Energy Accelerators, in Annual Review of Nuclear Science, Vol. 11, Annual Reviews, Palo Alto, 1961.

24. S. Kao and G. Voss, Effectiveness of Ilmenite-Loaded Concrete in Attenuating Neutron Radiation Produced by a 5 BeV Photon Beam, USAEC Report CEAL-1007, Cambridge Electron Accelerator, December 1963.

25. 200 BeV Accelerator Design Study, USAEC Report UCRL-16000, Lawrence Radiation Laboratory, June 1965.

26. G. N. Fowler and A. W. Wolfendale, The Interaction of μ-Mesons with Matter, in Progress in Elementary Particle and Cosmic Ray Physics, Vol. IV, North-Holland, Amsterdam, 1958.

27. L. Eyges, Multiple Scattering with Energy Loss, Phys. Rev. 74 : 1534 (1948)

28. These are the good geometry values which are given many places, for example, T. Rockwell III (Ed.), Reactor Shielding Design Manual, Van Nostrand, New York, 1956.

FIGURE CAPTIONS.

Fig. 1 Variation with Z of the nuclear removal mean free path, λ, radiation length, X_o, the radial distribution parameter, X_1, and the maximum photon mean free path, Λ; all in g/cm^2.

Fig. 2 Percent of energy absorbed beyond radius a, U(a), as a function of a/X_1. The points are from Monte Carlo calculations for the energies and materials indicated.

Fig. 3 Schematic of a typical shielding geometry.

Fig. 4 Total photonuclear cross section divided by atomic weight (mb/nucleon) as a function of photon energy.

Fig. 5 Neutron production by electrons and protons on copper as a function of neutron angle. The curves indicate the number of neutrons with energies greater than ϵ.

Fig. 6 Normalized radiation level ($r^2 D_P$ in Eq. 5) for $\theta = 0^\circ, 45^\circ, 90^\circ$, and 135° as a function of shield thickness, H, in feet of earth equivalent.

Fig. 7 Comparison of CEA shielding experiment with calculation.

Fig. 8 Integral muon yields as a function of normalized muon energy.

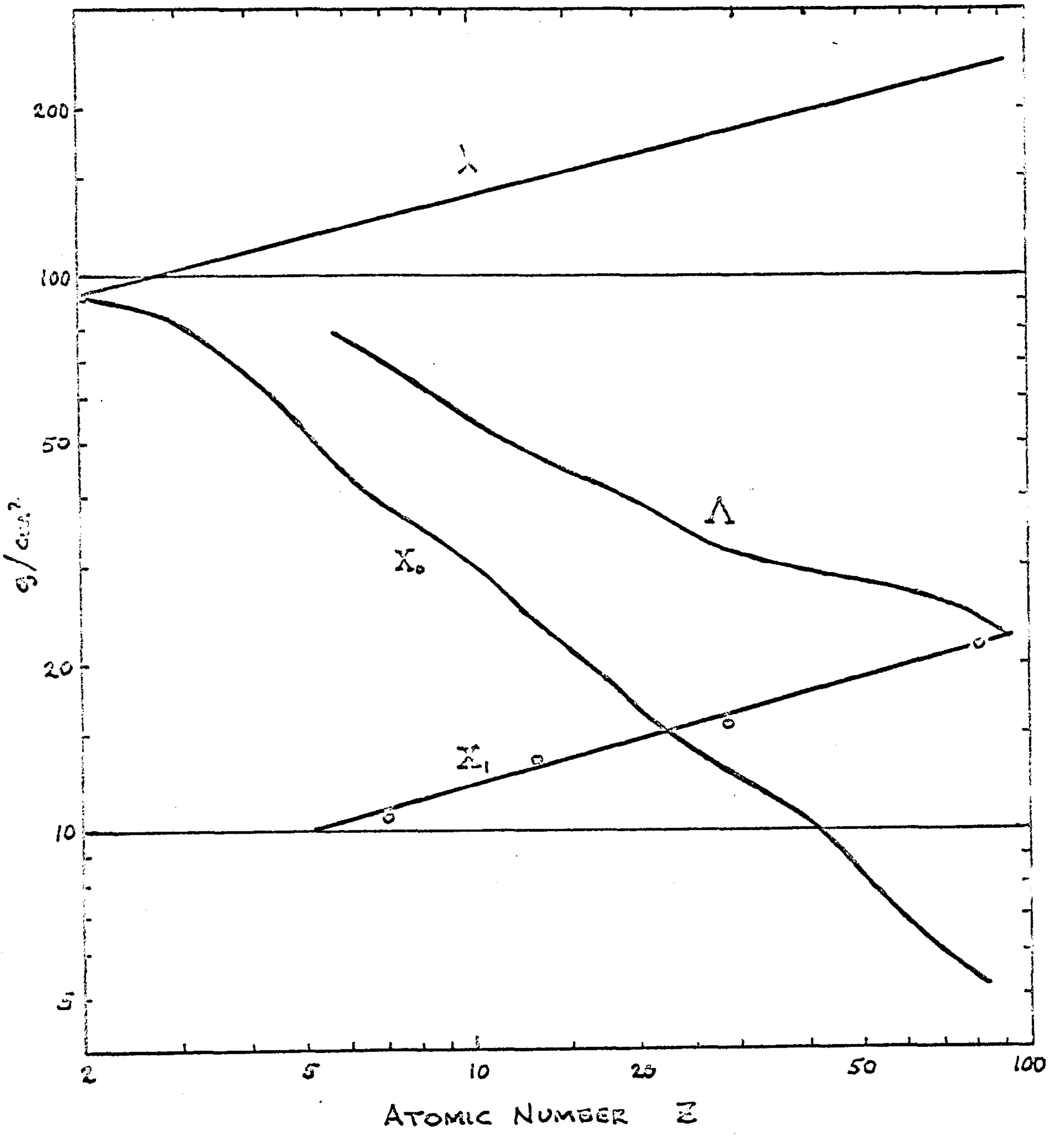

Figure 1

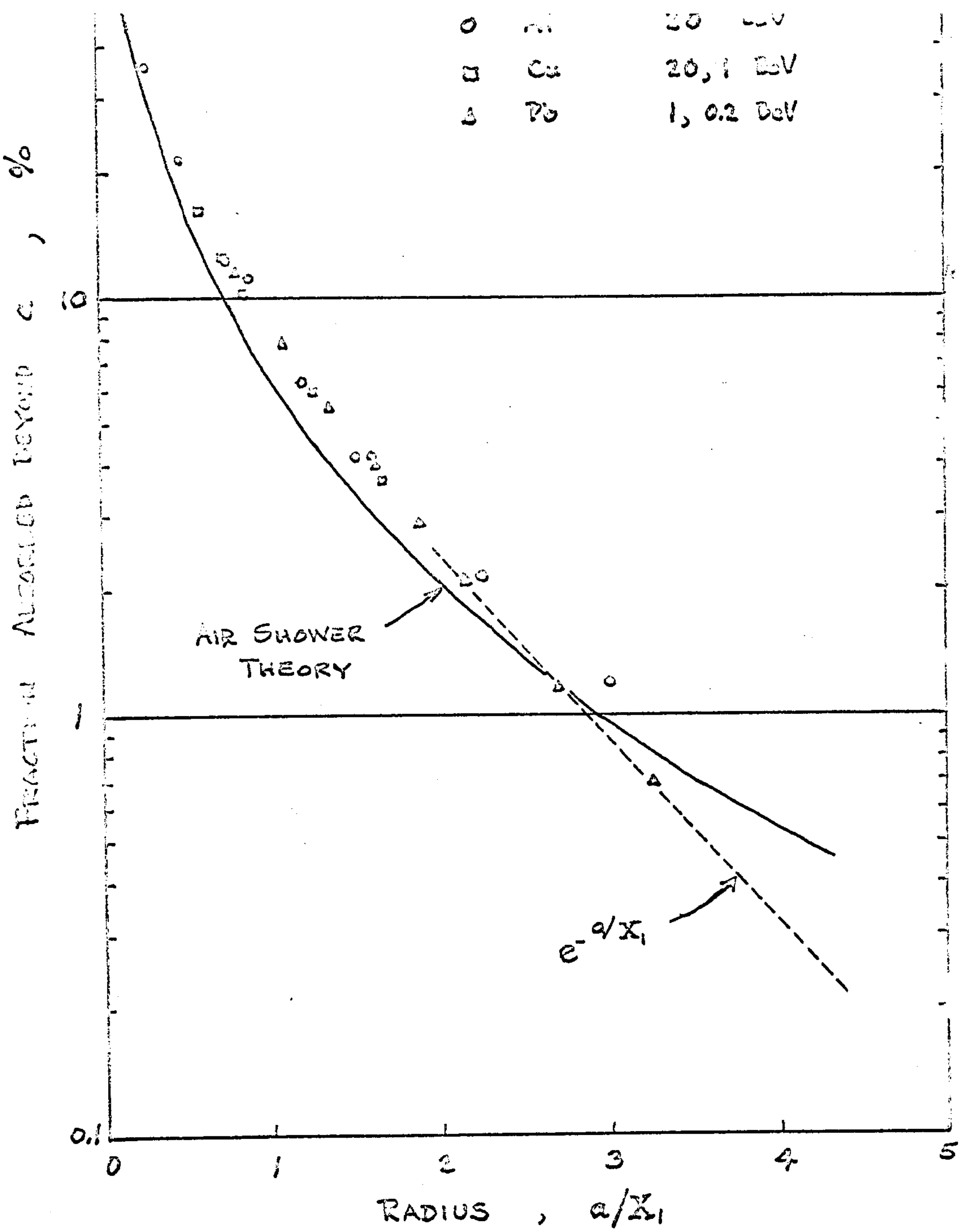
Cu 20, 1 BeV
Pb 1, 0.2 BeV
AIR SHOWER THEORY
e^{-a/X_1}
RADIUS , a/X_1
10
1
0.1
0
1
2
3
4
5

Figure 2

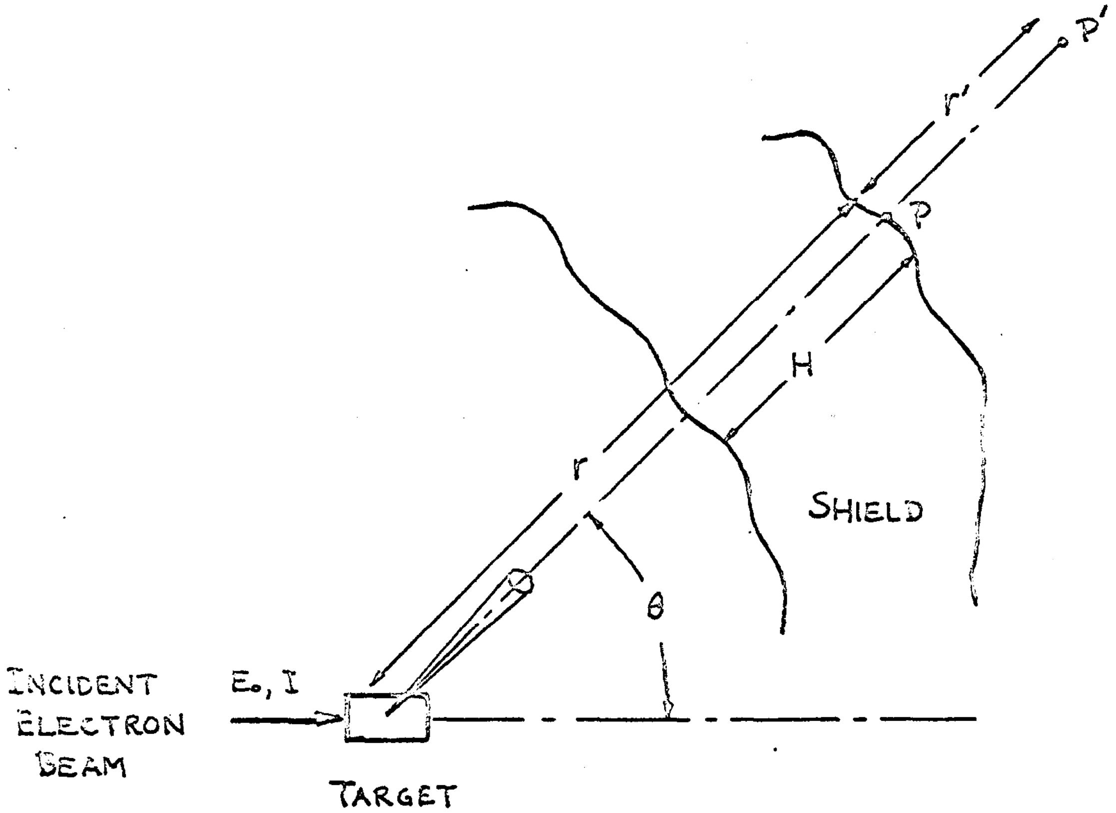

GENERAL LAYOUT

Figure 3

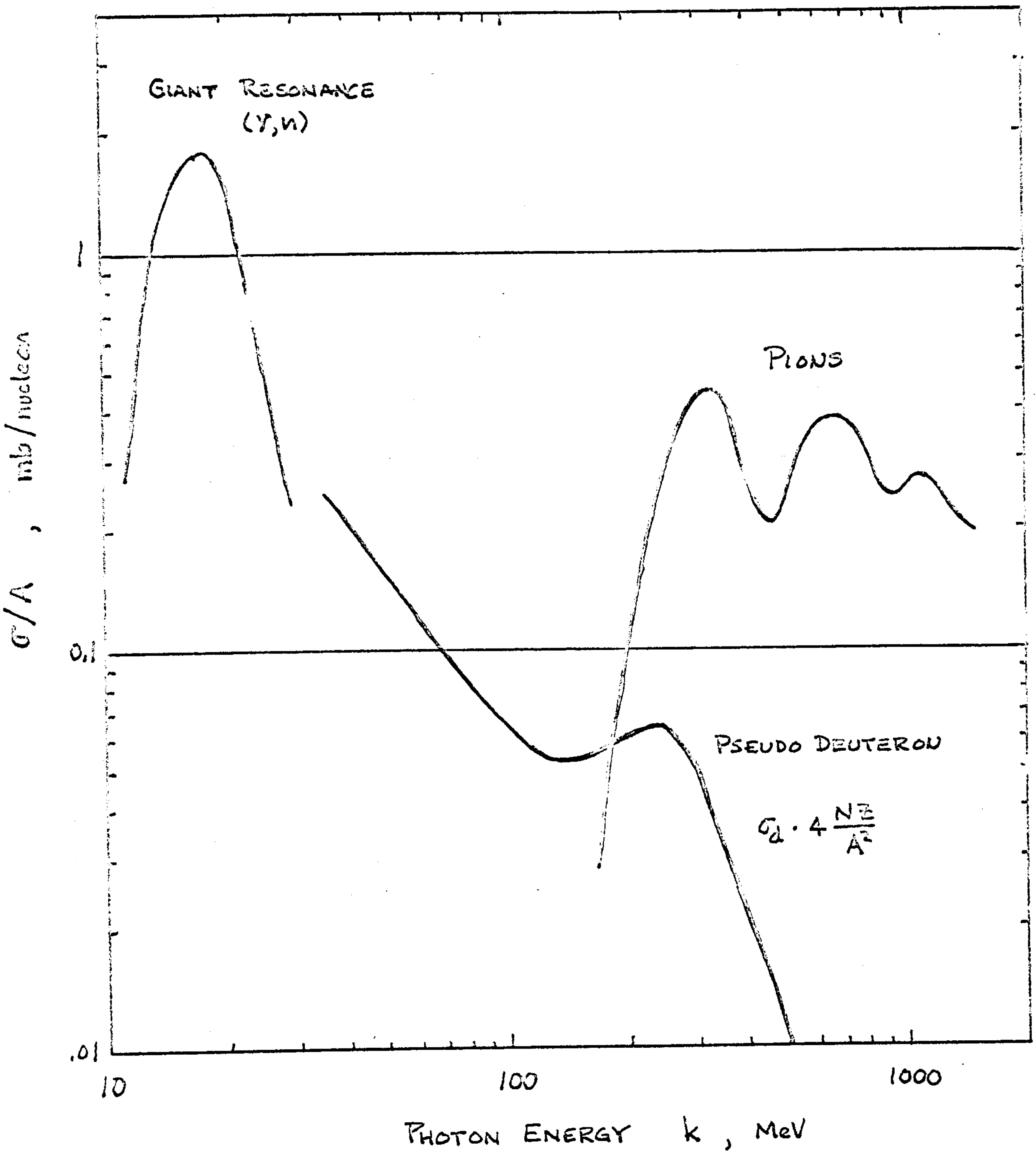
GIANT RESONANCE
(γ,n)
PIONS
PSEUDO DEUTERON
$\sigma_d \cdot 4\frac{NZ}{A^2}$
1
0.1
.01
10
100
1000
PHOTON ENERGY k , MeV
σ/A , mb/nucleon

Figure 4

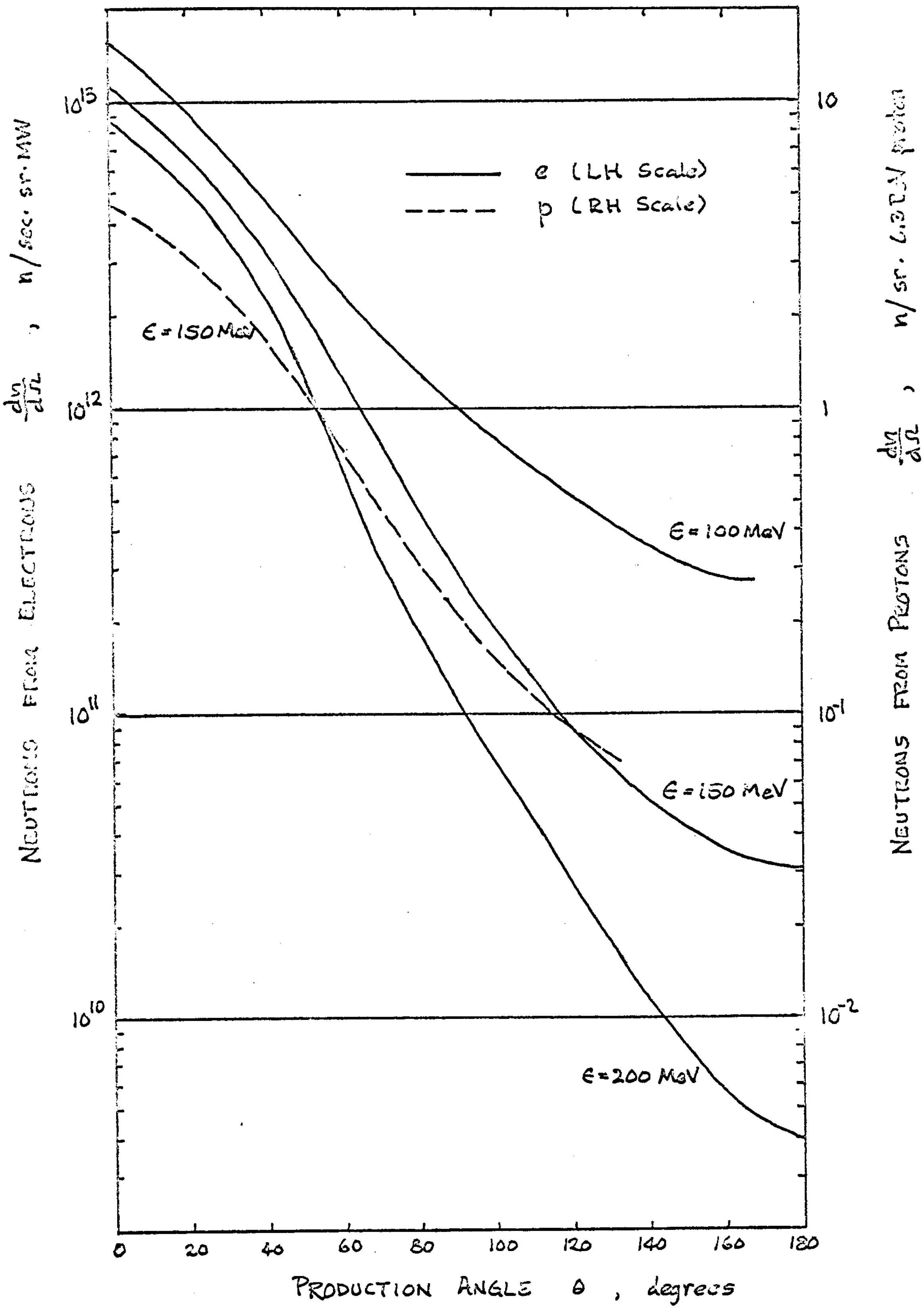
e (LH Scale)
p (RH Scale)
ε = 150 MeV
ε = 100 MeV
ε = 150 MeV
ε = 200 MeV
10^{15}
10^{12}
10^{11}
10^{10}
10
1
10^{-1}
10^{-2}
0
20
40
60
80
100
120
140
160
180
Production Angle θ, degrees
Neutrons from Electrons $\frac{dn}{d\Omega}$, n/sec·sr·MW
Neutrons from Protons $\frac{dn}{d\Omega}$, n/sr·

Figure 5

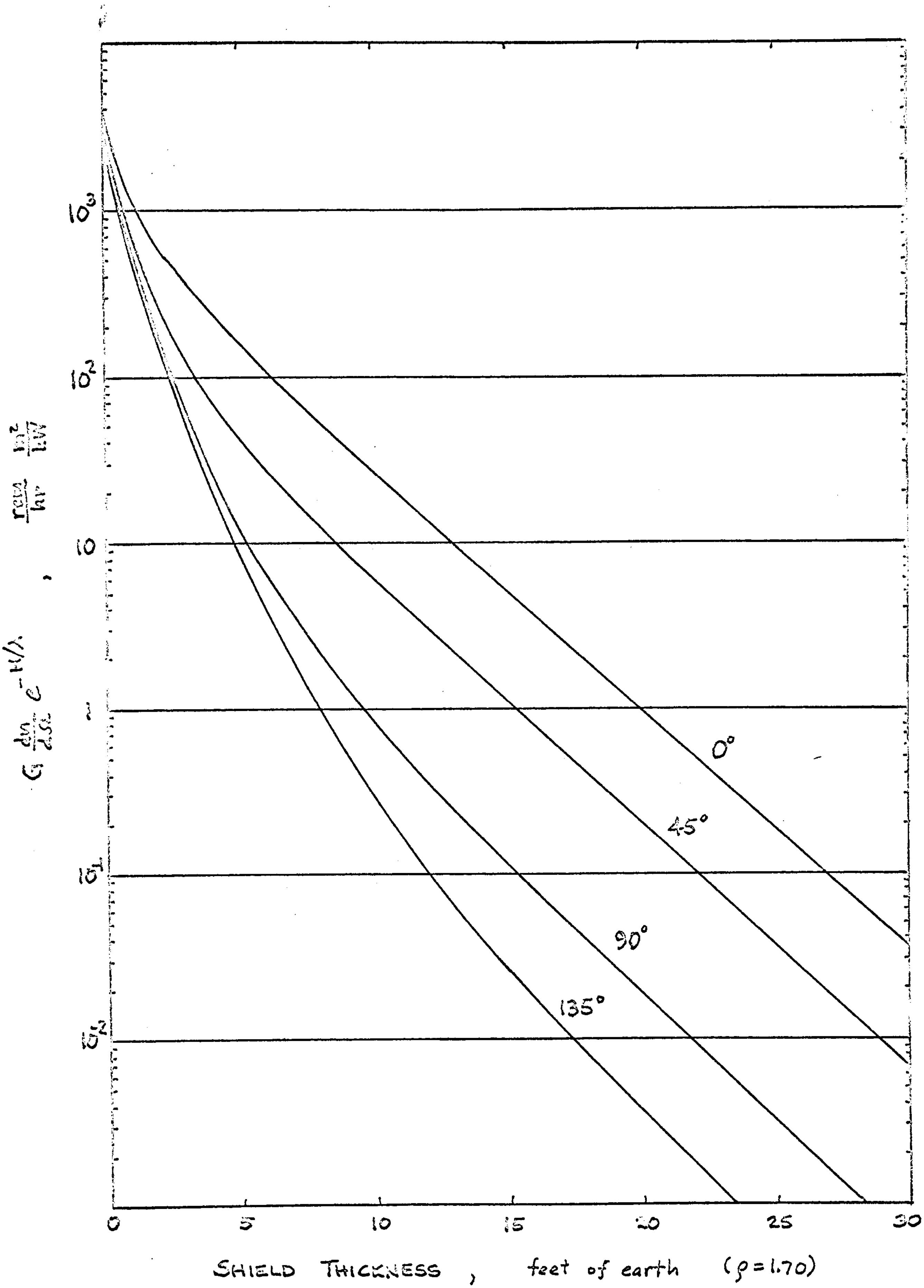

Figure 6

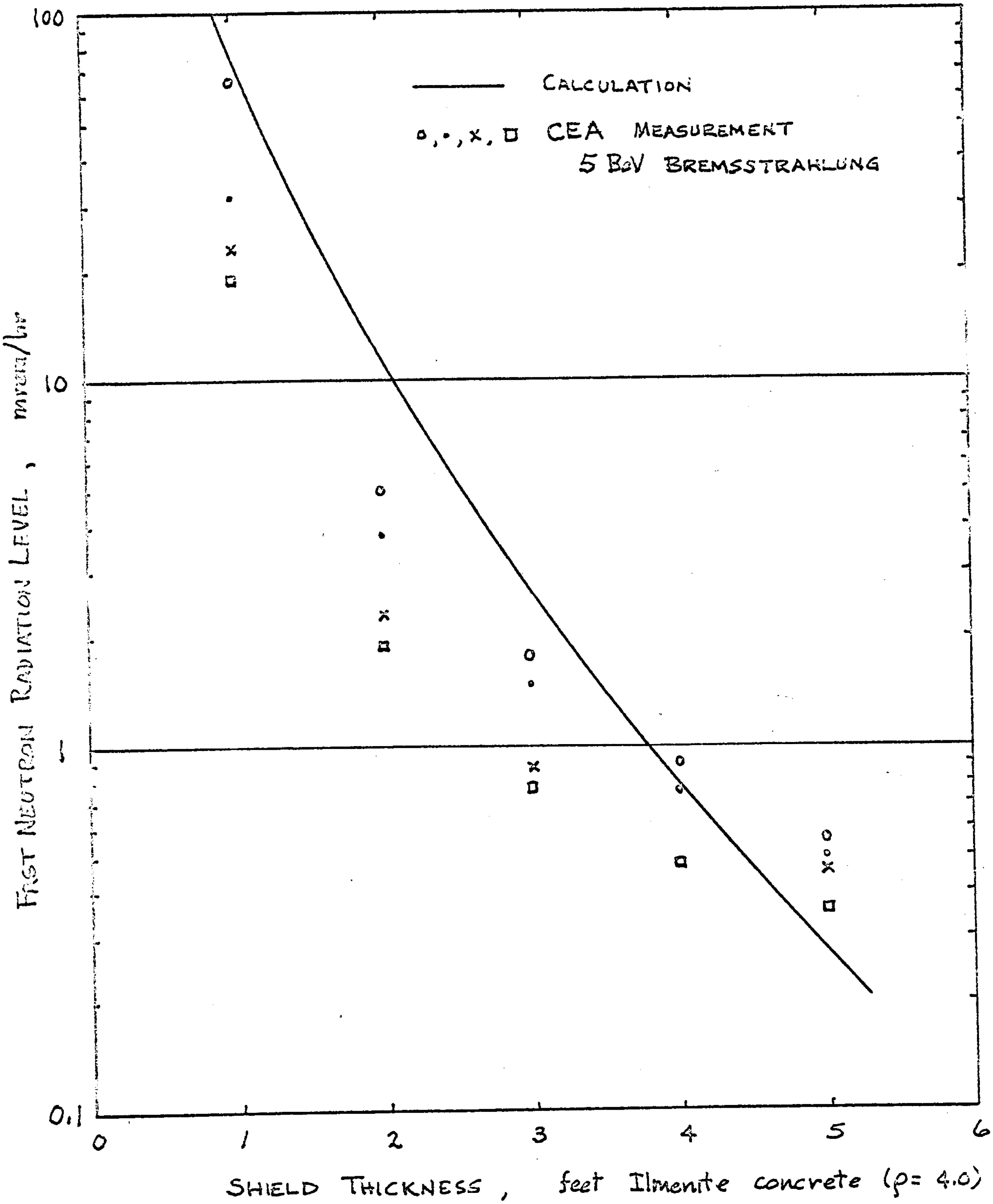

CALCULATION
o, •, x, □ CEA MEASUREMENT
5 BeV BREMSSTRAHLUNG
FAST NEUTRON RADIATION LEVEL, mrem/hr
SHIELD THICKNESS, feet Ilmenite concrete (ρ= 4.0)
100
10
1
0.1
0
1
2
3
4
5
6

Figure 7

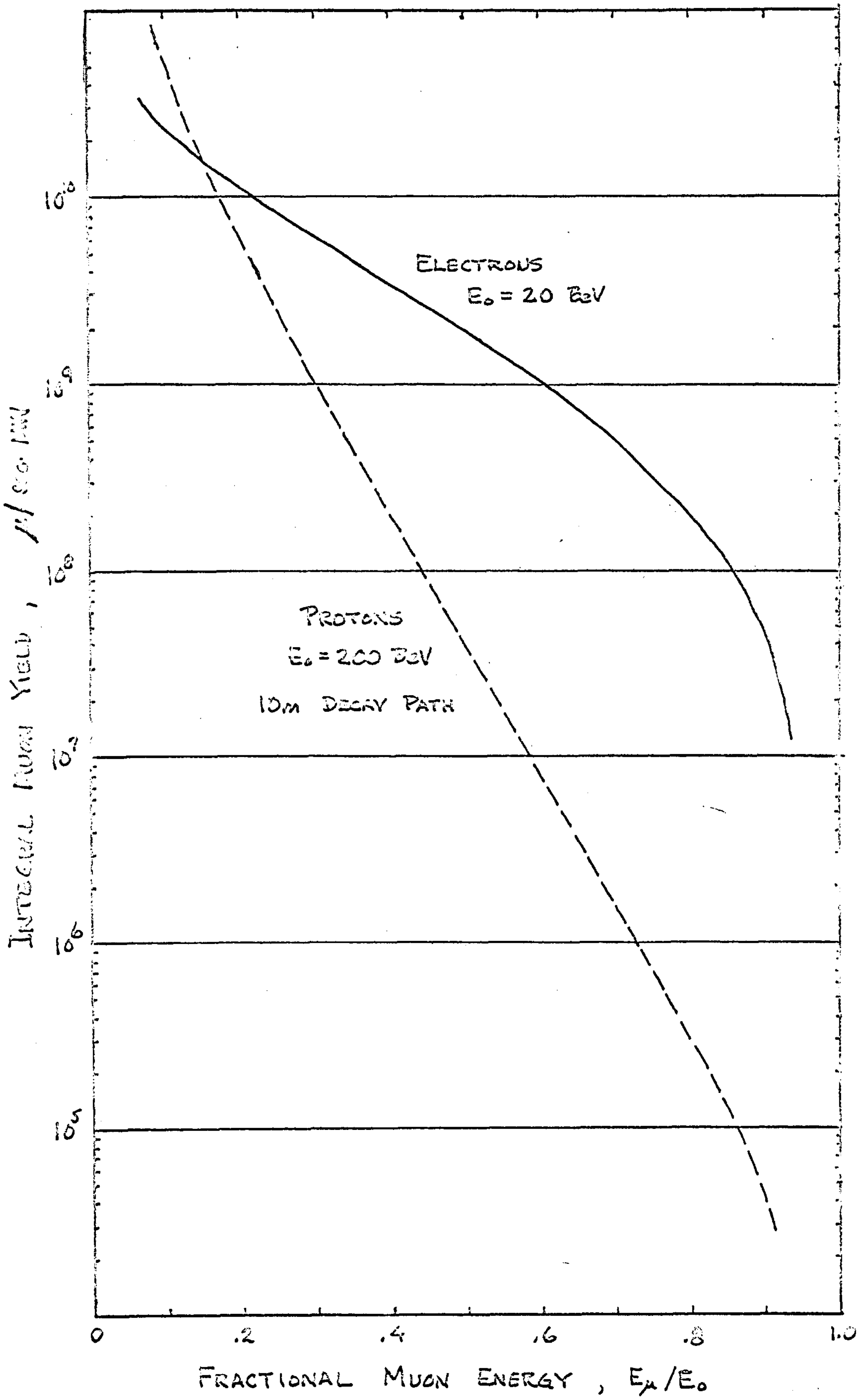

Electrons
$E_o = 20$ BeV
Protons
$E_o = 200$ BeV
10m Decay Path
10^{10}
10^9
10^8
10^7
10^6
10^5
Integral Muon Yield, μ/sec MW
0
.2
.4
.6
.8
1.0
Fractional Muon Energy, E_μ/E_o

Figure 8